5G NR-U: Homogeneous Coexistence Analysis

Siraj Muhammad, Hazem H. Refai
Electrical and Computer Engineering
University of Oklahoma
Tulsa, OK, USA
{sirajmuhammad, hazem}@ou.edu

Mohamad Omar Al Kalaa
Center for Devices and Radiological Health
U.S. Food and Drug Administration
Silver Spring, MD, USA
omar.al-kalaa@fda.hhs.gov

***Abstract*—Current technical reports indicate License-Assisted Access (LAA) Listen-Before-Talk (LBT) as the preferred channel access scheme for the upcoming 5G New Radio-Unlicensed. Various studies have examined heterogeneous coexistence of Wi-Fi/LTE-LAA systems. This paper investigates the homogeneous coexistence of intra-network LAA-LBT devices operating in dense deployment scenarios. Results relevant to ETSI-specified priority classes are reported in terms of channel utilization, collision probability, and channel access delay. The framework presented in this paper is then employed to investigate wireless coexistence in a 5G-enabled intensive care unit employing remote patient monitoring over 5G NR-U.**

***Index Terms*—LBT, 5G, NR-U, coexistence, e-health, wireless medical device**

I. Introduction

As the 3rd Generation Partnership Project (3GPP) continues the development of the fifth generation (5G) of mobile broadband standards, access to unlicensed spectrum in the Industrial, Scientific, and Medical (ISM) frequency bands has been under consideration under the name of 5G New Radio-Unlicensed (5G NR-U). Recently, there has been a push by the telecommunications industry to make portions of the 1200 megahertz in the 6 GHz (5.925-7.125 GHz) frequency band available for unlicensed use. 3GPP reports identify the channel access mechanism Listen-Before-Talk (LBT) used in LTE License-Assisted Access (LTE-LAA) as a baseline for use in the unlicensed spectrum including the prospected 6 GHz band [1]. The introduction of 5G in unlicensed spectrum may raise coexistence issues with incumbent Radio Access Technologies (RATs). Despite similarities with Wi-Fi's Enhanced Distributed Channel Access (EDCA), LBT received attention from the industry and academic research communities and led to the publication of many reports and articles detailing its coexistence characteristics. Numerous studies have been published on the feasibility of LBT-powered Long-Term Evolution (LTE) coexisting with Wi-Fi. However, degradation in performance can also arise in homogeneous networks employing a single technology. Accordingly, the LAA-LBT channel access mechanism in the unlicensed spectrum merits evaluation under homogeneous settings to understand its efficiency, fairness, and adaptability. Therefore, this paper investigates 5G NR-U coexistence without interference from other possible incumbent RATs.

Given the many applications being wirelessly connected in the era of the Internet of Things (IoT), certain vertical markets necessitate tight control of communications features, such as ultra-low-latency, high bandwidth, and massive density. An example could be remote pervasive monitoring in the home and hospital environments using 5G-enabled wearables and sensors to provide perpetual monitoring of patients' physiological measurements, e.g., respiratory effort, heart rate, and blood pressure [2]. Given the risk to patients associated with the delay or disruption of the wireless communication link, such medical applications have little tolerance to changes in connection reliability. This paper will develop an analytical model for LBT, validate it with simulation, and use it to investigate a hospital scenario implementing 5G NR-U in an Intensive Care Unit (ICU). We will investigate the four channel access priorities defined in the LBT specifications in single-class deployment, and assess the interplay of different class priorities on the overall channel efficiency, communication latency, and failure rate (collision probability) in multi-class scenarios.

The balance of this paper is organized as follows. Section II surveys the literature on channel access methods of LTE-LAA and Wi-Fi. Section III expounds standardized LBT according to the European Telecommunications Standards Institute (ETSI) regulations. The analytical model is developed in Section IV and homogeneous coexistence analysis is presented in Section V. A case study of an ICU scenario is investigated in Section VI and Section VII concludes the paper.

II. Related Work

Bianchi modeled the Distributed Coordination Function (DCF)—EDCA's precursor—using Markov chains [3]. Thereafter, Markov chains has been common in analytical assessment of similar channel access methods.

In [4] a Bianchi model was derived to analyze the priority schemes in 802.11 EDCA. Saturation throughput and delay were investigated for two of the four access categories defined in the standard (i.e., background, best effort, video, and voice). Mehrnoush et al. [5] studied the coexistence of LTE-LAA with Wi-Fi networks. Analysis was detailed by means of a Bianchi model variant and was validated by experimental simulation. Effect of energy detection threshold on throughput performance was investigated. The authors reported the impact of channel access parameters on the coexisting network, i.e., Wi-Fi or LTE-LAA. In technical specification 36.213 of release 13, 3GPP introduced a new channel access parameter dictating the number of retransmissions a station could perform on a maximum backoff stage before it is attempted again with the lowest backoff level. This new addition to the LTE-LAA standard was modeled in [6] and coexistence with Wi-Fi was examined, as well as the impact of the retransmission parameter. Hirzallah et al. [7] modeled LBT and EDCA channel access schemes with traffic priorities as a Markov chain, employing packet arrival rate and probability of saturation. An approximate closed form for the probability of successful transmission was derived as well. The authors simulated coexistence of LTE and Wi-Fi nodes each serving four priority-class queues. Coexistence was characterized in terms of achieved throughput, average contention delay, probability of successful transmission, and collision; all as a function of an equal number of LTE-LAA/Wi-Fi transmitters. LTE-LAA was assessed in [8] with respect to traffic priorities. Basic access and Request-to-Send/Clear-to-Send (RTS/CTS) mechanisms were examined. The paper addressed a mixed-priority case but only controlled the number of Class 2 nodes in the scenario. Co-channel coexistence was empirically evaluated for LTE-LAA and Wi-Fi in [9]. Achieved throughput was investigated for both networks during coexistence period, and channel occupancy of LTE-LAA system was measured for different Modulation and Coding Schemes (MCS) without Wi-Fi interference.

Quality literature have addressed many topics pertaining to LBT including coexistence with Wi-Fi and enhancing the performance therein. With the exception of [10] on EDCA and [8] on LBT, most of the reviewed work overlooked a same-technology analysis with respect to multi-class scenarios. Furthermore, yet to be reported is a comprehensive overview of the interplay of different class priorities and the impact of multi-class deployment on the overall channel efficiency and per-node delay. We address this gap in this paper with the aim of understanding future 5G NR-U behavior in scenarios with high demand for communication reliability like the use of 5G in healthcare. We also expect that our study will inform the development of a more efficient channel access mechanisms for 5G NR-U wireless systems and their operation in the potential new 6 GHz unlicensed band.

III. Listen-Before-Talk

Notably, 3GPP had two versions of LBT proposed in their technical reports and specifications. The first was introduced in TR 36.889 [11] in 2015 was not compliant with the regulations set forth later by ETSI in 2017. In EN 301 893 [12], ETSI formally detailed the LBT mechanism that was later adopted by 3GPP in TS 36.213 [13] in 2017 to make LTE-LAA amenable for deployment in the unlicensed spectrum. However, the majority of research disseminated on this topic relied on the old non-standardized version of LBT.

This paper is focused on the standardized version of LBT as stipulated in ETSI's regulations. The mechanism is purposed to detect other in-band RATs transmissions and refrain from interfering with them while the detected power is above a predefined threshold. Additionally, the standard defines four sets of channel access parameters assigned to data packets that determine the contention behavior on the channel and the duration for which they are allowed to endure. Accordingly, high priority packets are more likely to gain access but must have a shorter duration. Table I lists the parameters of these classes with 4 being the highest priority class and 1 is the lowest. Channel Occupancy Time (COT) is the maximum time not to be exceeded by nodes when utilizing the channel. The value of P0 and contention window sizes are given in terms of the number of observation slots. Note that the standard allows Class 1 and 2 to increase their COT to 8 ms given that pauses of at least 100 μs are inserted during transmission.

TABLE I
LBT class priorities defined in the ETSI standard.

Class	P0	CW_{min}	CW_{max}	COT [ms]
4	1	4	8	2
3	1	8	16	4
2	3	16	64	6⋆
1	7	16	1024	6⋆

⋆can extend to 8 ms if transmission includes 100 μs pauses

The LBT procedure starts with a waiting period equal to 16 μs referred to as Short Inter-Frame Spacing (SIFS). Followed by the prioritization period (P0 in Table I), the value of which is determined by the packet class. P0 is a Clear Channel Assessment (CCA) period that is used to determine the channel state (idle or busy) and differentiates between frame types; low priority frames wait for longer P0 periods. When both of SIFS and P0 expire without detecting any channel activities registered above the Energy Detection (ED) threshold, the equipment may start the contention process; i.e., each observation slot in SIFS and P0 must pass a CCA. Subsequently, the backoff mechanism starts by initializing the channel access parameters, which are also determined by the priority class of traffic. This comprises setting the contention window CW to its minimum value CW_{min} and drawing a random number q between 0 and $CW-1$. The value of q is the number of time slots the equipment needs to implement CCA for. During a single observation slot, the channel is considered occupied if transmissions were detected with a level above the ED threshold. In which case, the LBT procedure starts anew with the SIFS period. Otherwise, the value of q is decremented by exactly one. If q reaches 0, the device gains access to the channel and may transmit. Afterwards, if a transmission fails, the device may attempt a retransmission after adjusting its contention window size. CW is set to $2^i CW$ where i is the backoff stage; i.e., the contention window is doubled until it reaches the frame's maximum value CW_{max}. Fig. 1 illustrates this procedure in a flowchart (see Annex F in [12] for an expanded chart).

IV. System Model

The channel access model of LBT used herein follows Bianchi's model [3]. Assuming n_c stations operate in a

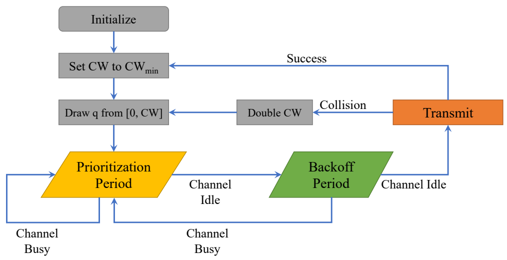

Fig. 1. A high-level flowchart demonstrates the LBT procedure for Frame Based Equipment as stipulated in ETSI standard.

saturation condition, a station always has data to transmit, and consequently is always trying to access the channel. Ideal channel conditions are assumed as well. Additionally, the model postulates that each station has a single class of traffic to send per Table I; i.e., each station represents one priority class $c \in \mathcal{C} = \{1, 2, 3, 4\}$, and exhibits a constant collision probability p_c that is independent of retransmissions. Probability of transmission for a station of class c is given in [3]:

$$\tau_c = \frac{(1 - 2p_c)}{(1 - 2p_c)(W_c + 1) + p_c W_c (1 - (2p_c)^{m_c})}, \quad (1)$$

where W_c is the minimum contention window size of class c; m_c is the maximum backoff stage of class c. p_c is the probability that at least one of the remaining $n_c - 1$ stations transmit concurrently:

$$p_c = 1 - (1 - \tau_c)^{n_c - 1}. \quad (2)$$

In a homogeneous scenario where all nodes are of the same class, let γ_c be the probability that at least one station of class c transmits:

$$\gamma_c = 1 - (1 - \tau_c)^{n_c}. \quad (3)$$

Then, the probability that a successful transmission of class c occurs on the channel is given by conditioning the probability that *exactly one* station transmits by the probability that *at least one* station transmits:

$$\rho_c = \frac{n_c \tau_c (1 - \tau_c)^{n_c - 1}}{\gamma_c}. \quad (4)$$

Let ψ_c be the Effective Channel Utilization (ECU) of class c, defined as the ratio of time the channel is used to successfully transmit packets of class c over the average channel time. Hence,

$$\psi_c = \frac{\gamma_c \rho_c T_c}{(1 - p_c)\sigma + \gamma_c \rho_c T_c + \gamma_c (1 - \rho_c) T_c}, \quad (5)$$

where σ is the unit time slot duration (observation slot), and $T_c = COT$ is the maximum class occupancy time. Average channel time in the denominator accounts for idle time slots that occur with probability $1 - p_c$; successful transmission slots, with probability $\gamma_c \rho_c$; and collisions, with probability $\gamma_c (1 - \rho_c)$. The model was validated using a stochastic simulator written in C++. Fig. 2a depicts the ECU

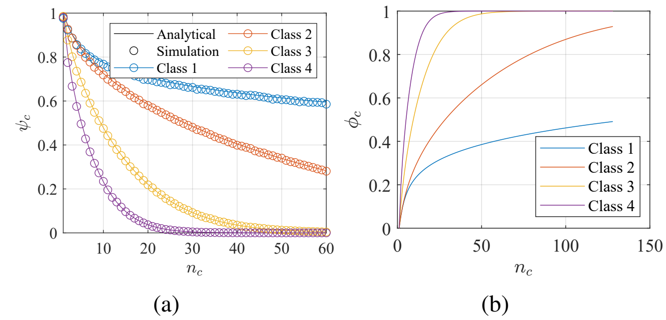

Fig. 2. (a) ECU vs. number of contending nodes in homogeneous class setting, for both, analytical and simulation results. (b) Channel collisions as a function of the contending nodes number for all four priority classes sharing the channel homogeneously.

obtained from the simulator and equation (5) of the analytical model. It shows the channel utilization during homogeneous coexistence of different priority classes, each with a varying number of contending nodes n_c. The accuracy of the Discrete-Time Markov Chain (DTMC) model is noted where the analytical results represented by solid lines significantly overlap with simulation results illustrated by round markers. All simulation results were obtained from independent runs of the simulator equivalent to 200 seconds of air time. Microsecond-precision statistics on idle time, successful transmission time, and collision time were collected to calculate corresponding metrics.

V. Coexistence Analysis

A. One-Class Dense Deployment

ECU is defined as the percentage of aggregate time the channel is occupied to successfully transmit packets by any coexisting station. If a station successfully completes a transmission, then it has occupied the channel for a period of COT pertaining to its class without colliding with another station's transmission. ECU illustrates the extent to which the channel is efficiently utilized without collisions. Fig. 2a presents a typical dense deployment of a future 5G NR-U network. Results indicate that ECU significantly declines as the number of contending stations increases. Classes 3 and 4 exhibit an inferior performance compared to the two lower priority types; Class 2 drops well below 50% after 30 devices start sharing the channel. In contrast, at 20 nodes, ECU of Classes 3 and 4 drops to 22% and 3.7%, respectively. Since saturation conditions are assumed, idle times have a negligible effect on channel utilization. This observation suggests that the decline in ECU is attributed to collisions on the channel.

Let ϕ_c denote the normalized time during which collisions from traffic of priority class c can be observed on the channel. Then, similar to the definition of ψ_c in (5), ϕ_c is defined as

$$\phi_c = \frac{\gamma_c (1 - \rho_c) T_c}{(1 - p_c)\sigma + \gamma_c \rho_c T_c + \gamma_c (1 - \rho_c) T_c}. \quad (6)$$

Fig. 2b plots the percentage of channel collisions for each priority class as a function of the number of contending stations. The plot corroborates that under saturation condition

ψ_c and ϕ_c compose the majority of channel time, while idle time slots are insignificant. Consequently, deteriorating ECU is attributed to channel collisions. We study a homogeneous case with ideal channel assumptions. Accordingly, collisions can be attributed to multiple nodes choosing the same counter value during backoff procedure after the channel becomes idle. When their counters expire, they transmit simultaneously, which results in a collision. Given that Class 3 and Class 4 exhibit smaller contention window sizes, they are more susceptible to intra-network collisions (i.e., within networks of the same class) than the other two priority types.

To calculate the mean access delay D_c for all contending nodes in the channel, we leverage a property of ergodic Markov chains that relates steady-states probabilities with mean recurrence times in an inversely proportional relation [14],

$$D_c = \frac{n_c T_c}{\psi_c}. \tag{7}$$

B. Two-Class Deployment Scenario

In this section, analytical expressions for multi-class scenario are developed for the ECU, collision probability, and mean access delay. Each class is treated as a separate system with an independent transmission probability τ_c. Therefore, the conditional probability of collisions p_c is revised to account for other stations serving different frame types. Accordingly, eq. (2) becomes:

$$p_c = 1 - (1-\tau_c)^{n_c - 1} \prod_{k \in \mathcal{C}, k \neq c} (1-\tau_k)^{n_k}. \tag{8}$$

Similarly, ψ_c given in (5) becomes:

$$\psi_c = \frac{\gamma_c \rho_c T_c \prod_{k \in \mathcal{C}, k \neq c} (1-\gamma_k)}{T_N}. \tag{9}$$

T_N represents the normalized time which accounts for every possible event that could happen on the channel. It consists of idle slots, successful transmissions, and multi-node transmissions (i.e., collisions).

$$\begin{aligned} T_N = {} & (1-\gamma_{c_a})(1-\gamma_{c_b})\sigma + (\gamma_{c_a}\rho_{c_a})(1-\gamma_{c_b})T_{c_a} + \\ & \gamma_{c_a}(1-\rho_{c_a})(1-\gamma_{c_b})T_{c_a} + (1-\gamma_{c_a})(\gamma_{c_b}\rho_{c_b})T_{c_b} + \\ & (\gamma_{c_a}\rho_{c_a})(\gamma_{c_b}\rho_{c_b}) \min(T_{c_a}, T_{c_b}) + \\ & \gamma_{c_a}(1-\rho_{c_a})(\gamma_{c_b}\rho_{c_b})T_{c_a} + (1-\gamma_{c_a})\gamma_{c_b}(1-\rho_{c_b})T_{c_b} \\ & + (\gamma_{c_a}\rho_{c_a})\gamma_{c_b}(1-\rho_{c_b})T_{c_b} + \\ & \gamma_{c_a}(1-\rho_{c_a})\gamma_{c_b}(1-\rho_{c_b}) \max(T_{c_a}, T_{c_b}). \end{aligned} \tag{10}$$

The total ECU $\psi = \psi_{c_a} + \psi_{c_b}$ for adjacent priorities (i.e. coexisting networks priorities c_a and c_b differ in one level) is depicted in Fig. 3. The inner edges of the plots report the ECUs discussed in Fig. 2a previously, since they correspond to single-class situations. As more nodes of higher priorities are added to the channel, total ECU significantly drops because of increased collisions. This can be noticed in Fig. 3a and 3b which demonstrate total ECU for Classes 1-2, and 2-3, respectively. For the case of Class 3 and Class 4 networks

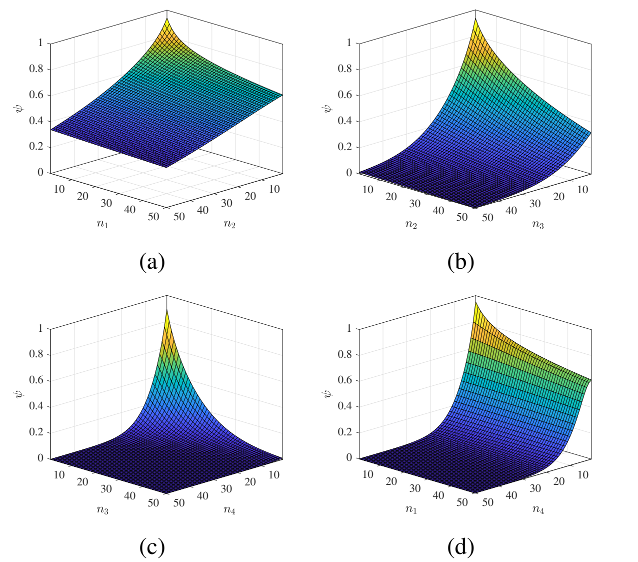

Fig. 3. Aggregate ECU for different combinations of priority classes: (a) Class 1 and Class 2, (b) Class 2 and Class 3, (c) Class 3 and Class 4, (d) Class 1 and Class 4.

depicted in Fig. 3c, ECU acutely drops due to adverse effect of collisions in both types. Because of the similarities in the parameters of their backoff procedure, both classes contribute almost equally to the degradation of total channel ECU. The degradation is associated with higher priority class on the channel. To better illustrate this observation, consider another scenario of Classes 1 and 4 shown in Fig. 3d. This case further elucidates that remark because of disparity in coexisting priority levels. Class 1 nodes do not influence the channel as much as Class 4, as the number of nodes increases. For example, the ECU of five Class 1 and a single Class 4 nodes is approximately 85%. Adding five more Class 4 stations brings the total ECU down to 50.44%. In contrast, 50.54% ECU for a single Class 4 device drops to 46.33% ECU with a ten times denser network of fifty Class 1 nodes. This influence of Class 1 network subsides as more devices of the higher priority join the channel and become the predominant variable affecting the total channel efficiency.

The developed analytical model makes it possible to analyze and break down collisions that occur during class-heterogeneous deployments. We will address collisions in two-class scenarios as a three-component metric: intra-network (one for each priority class) and inter-network collisions. For a two-class scenario c_a and c_b with a number of nodes n_{c_a} and n_{c_b}, respectively, collision probabilities are given as follows:

$$\begin{aligned} \phi_{c_a} &= \frac{\gamma_{c_a}(1-\rho_{c_a})(1-\gamma_{c_b})T_{c_a}}{T_N} \\ \phi_{c_b} &= \frac{\gamma_{c_b}(1-\rho_{c_b})(1-\gamma_{c_a})T_{c_b}}{T_N} \\ \phi_{c_a c_b} &= (T_C - \gamma_{c_a}(1-\rho_{c_a})(1-\gamma_{c_b})T_{c_a} - \\ & \quad \gamma_{c_b}(1-\rho_{c_b})(1-\gamma_{c_a})T_{c_b})/T_N, \end{aligned} \tag{11}$$

where T_C is the portion of normalized time which relates to

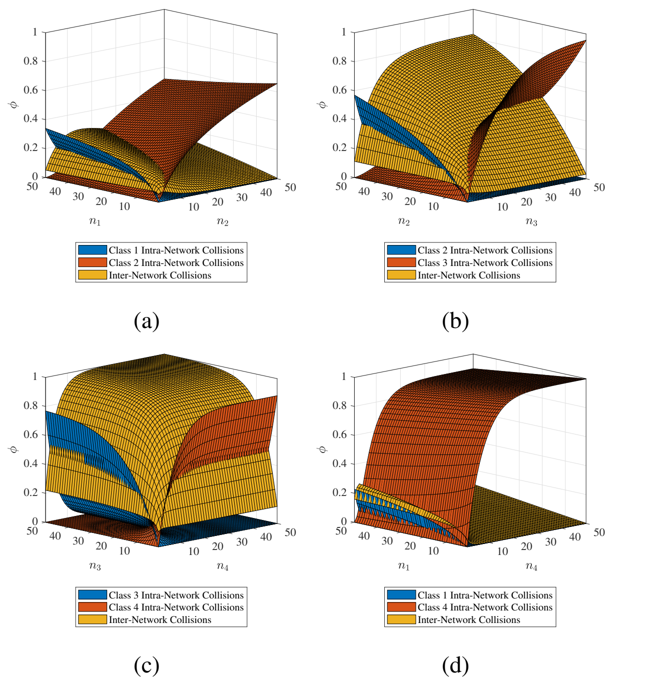

Fig. 4. Intra-network and inter-work collisions for different combinations of coexisting priority classes.

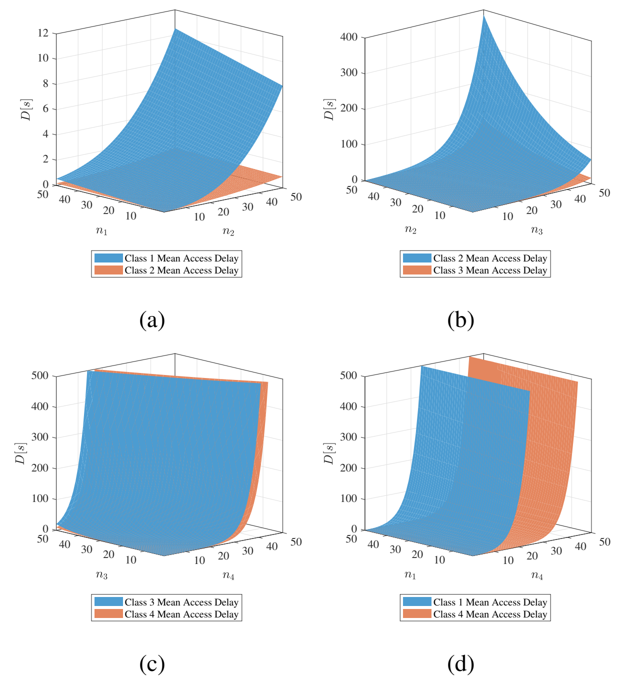

Fig. 5. Mean access delay for different combinations of coexisting priority classes.

collisions in eq. (10).

These expressions are plotted in Fig. 4 for various combinations of c_a and c_b. Consistent with our findings from previous discussion on ECU, Class 1 and Class 2 broadly exhibit fewer collisions than other higher levels of priority, as can be seen in Fig. 4a. This explains the higher ECU in this scenario; which is attributed to the wide range of backoff values these two classes incorporate in their procedure. Notably, inter-network collisions make as much as 28% of the time when the channel has between 5 and 25 stations of Class 2. After this limit, the bulk of collisions are ascribed to the higher priority in the medium, Class 2.

Fig. 4b and 4c show a different pattern with Classes 2-3, and 3-4, respectively. Intra-network collisions hinder the channel when one class has more nodes than the other. However, Fig. 4b suggests that this component is still responsible for up to 60% of the collisions in Class 2, and up to more than 90% of the collisions in Class 3. As more stations share the channel, inter-network collisions start to increase gradually until they become dominant over intra-network components. The rate at which the inter-network collisions escalates depends on the class and number of stations added to the channel. Fig. 4a and 4b demonstrate this behavior. Since Class 3 and Class 4 have similar contention parameters, they equally share the responsibility of collisions. Fig. 4c shows that their intra-network components are almost the same, with Class 4 slightly exceeding Class 3, while the major part of collisions is attributed to inter-network component.

In terms of mean access delay for the two-class case, Fig. 5 suggests that high priority classes incur more negative effect on lower class networks than they do among their nodes. This behavior is attributed to the fact that high levels of priorities cause more channel collisions, as discussed before. In addition to their significant likelihood of accessing the channel that stems from their small contention windows, they yield little time for lower priorities to transmit. Therefore, low priority class stations sustain longer delays than higher classes when coexisting heterogeneously.

VI. Case Study: Intensive Care Unit (ICU)

The number of ICU beds with full remote vital readings is expected to be around 100 by 2035 [15], and given the limited hospital area the high density of connections required to monitor patients could pose challenges to wireless networks [2]. The AAMI TIR69—Risk Management of Radio-Frequency Wireless Coexistence for Medical Devices and Systems [16]—specifies four risk categories for the wireless function of medical devices listed in Table II. The analysis presented hereafter could inform the design, development, and deployment of 5G-enabled healthcare applications. Assume an ICU environment with 75 active connections distributed across 25 beds belonging to AAMI TIR69 risk categories A, B, and C—25 connections for each. Expressions (8) and (9) can be expanded to reflect a three-class scenario. Assuming that the latency incurred by connections is equal to only the mean access delay, we estimate the time delay behavior in this scenario using (7).

3GPP permits manufacturers to assign packet priorities regardless of the payload type. Mapping risk categories to various frame priority classes and plotting mean access delay results in Fig. 6. We assume that class priorities 2, 3, and

TABLE II
AAMI TIR69 RISK CATEGORIES.

Category	Risk and result of failure, disruption, or delay of wireless communication
Category A	High Risk Level: could result in death or serious injury
Category B	Medium Risk Level: could result in injury or impairment requiring professional medical intervention
Category C	Low Risk Level: could result in temporary injury or impairment not requiring professional medical intervention
Category D	No Significant Risk Level: could result, as a maximum, in inconvenience or temporary discomfort

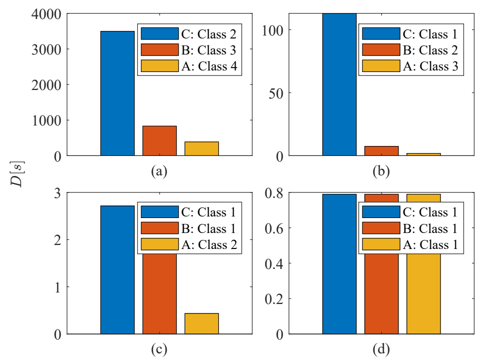

Fig. 6. Latency of connections in ICU environment mapped to various frame priority classes. (a) 2, 3, 4; (b) 1, 2, 3; (c) 1, 1, 2; (d) 1, 1, 1

4 are mapped to connections of risk categories C, B, and A. Accordingly, we note the elevated connection latency associated with connections of risk categories B and C as shown in Fig. 6a. Even for a type A connection, the average delay sustained is around 380 s. Designing functions with risk categories A, B, C to transmit using priority classes 3, 2, 1, respectively improves the latency by orders of magnitude as illustrated in Fig. 6b. Another design choice could be to cluster the connection types into two groups. For example, categories C and B could be assigned one class priority while category A is given a higher one as depicted in Fig. 6c. Using priority classes 2 and 3 improves over the previous three-class assignment; more so with lower priorities 1 and 2, reducing the latency to less than 3 seconds for categories C and B and less than 1 second for category A. Additionally, in case that high priority classes are guaranteed to be absent, one-class mapping can offer lower latency, as shown in Fig. 6d. This example highlights the importance of carefully designing the wireless function of the medical device to achieve the intended functionality in the use environment.

VII. CONCLUSION

Literature reports on cross-technology wireless coexistence analysis are many. This paper revisits the LBT channel access scheme and assesses its performance in a homogeneous setting without interference from other possible coexisting technologies. A Markov chain was used to model the LBT mechanism and its frame priority classes according to ETSI's regulations. ECU, collisions, and mean access delay were investigated for single-class and multi-class deployment scenarios. Finally, a case study on 5G NR-U-enabled ICU hospital environment was presented to highlight how the selection of channel access parameters can impact the wireless coexistence of 5G-enabled medical devices with diverse risk profiles when operating in the unlicensed spectrum.

DISCLAIMER

The mention of commercial products, their sources, or their use in connection with material reported herein is not to be construed as either an actual or implied endorsement of such products by the Department of Health and Human Services.

REFERENCES

[1] 3GPP, "Study on NR-based access to unlicensed spectrum, document TR 38.889 V16.0.0," Tech. Rep., 2018.

[2] G. Cisotto, E. Casarin, and S. Tomasin, "Requirements and Enablers of Advanced Healthcare Services over Future Cellular Systems," *IEEE Communications Magazine*, vol. 58, no. 3, pp. 76–81, mar 2020.

[3] G. Bianchi, "Performance analysis of the IEEE 802.11 distributed coordination function," *IEEE Journal on Selected Areas in Communications*, vol. 18, no. 3, pp. 535–547, mar 2000.

[4] Y. Xiao, "Performance analysis of priority schemes for IEEE 802.11 and IEEE 802.11e wireless LANs," *IEEE Transactions on Wireless Communications*, vol. 4, no. 4, pp. 1506–1515, jul 2005.

[5] M. Mehrnoush, V. Sathya, S. Roy, and M. Ghosh, "Analytical Modeling of Wi-Fi and LTE-LAA Coexistence: Throughput and Impact of Energy Detection Threshold," *IEEE/ACM Transactions on Networking*, vol. 26, no. 4, pp. 1990–2003, aug 2018.

[6] N. Bitar, M. O. Al Kalaa, S. J. Seidman, and H. H. Refai, "On the Coexistence of LTE-LAA in the Unlicensed Band: Modeling and Performance Analysis," *IEEE Access*, vol. 6, pp. 52 668–52 681, 2018.

[7] M. Hirzallah, M. Krunz, and Y. Xiao, "Harmonious Cross-Technology Coexistence With Heterogeneous Traffic in Unlicensed Bands: Analysis and Approximations," *IEEE Transactions on Cognitive Communications and Networking*, vol. 5, no. 3, pp. 690–701, sep 2019.

[8] Y. Ma, "Analysis of Channel Access Priority Classes in LTE-LAA Spectrum Sharing System," in *2018 27th International Conference on Computer Communication and Networks (ICCCN)*, vol. 2018-July. IEEE, jul 2018, pp. 1–7.

[9] M. O. A. Kalaa and S. J. Seidman, "Wireless Coexistence Testing in the 5 GHz Band with LTE-LAA Signals," in *2019 IEEE International Symposium on Electromagnetic Compatibility, Signal & Power Integrity (EMC+SIPI)*. IEEE, jul 2019, pp. 437–442.

[10] Z. Kong, D.-K. Tsang, B. Bensaou, and D. Gao, "Performance Analysis of IEEE 802.11e Contention-Based Channel Access," *IEEE Journal on Selected Areas in Communications*, vol. 22, no. 10, pp. 2095–2106, dec 2004.

[11] 3GPP, "Study on Licensed-Assisted Access to Unlicensed Spectrum, document TR 36.889 V13.0.0," The 3rd Generation Partnership Project (3GPP), Tech. Rep., 2015.

[12] ETSI, "Harmonised European Standard EN 301 893," Tech. Rep., 2017. [Online]. Available: http://www.etsi.org/deliver/etsi{_}en/301800{_}301899/301893/02.01.01{_}60/en{_}301893v020101p.pdf

[13] 3GPP, "Evolved Universal Terrestrial Radio Access (E-UTRA) Physical Layer Procedures, document TS 36.213 V13.6.0," 3GPP, Tech. Rep., 2017.

[14] G. Bolch, S. Greiner, H. de Meer, and K. S. Trivedi, *Queueing Networks and Markov Chains*, 2nd ed. New York, USA: John Wiley & Sons, Inc., aug 1998.

[15] C. Thuemmler, A. Paulin, and A. K. Lim, "Determinants of next generation e-Health network and architecture specifications," in *2016 IEEE 18th International Conference on e-Health Networking, Applications and Services, Healthcom 2016*. Institute of Electrical and Electronics Engineers Inc., nov 2016.

[16] AAMI, "AAMI TIR69:2017; Risk management of radio-frequency wireless coexistence for medical devices and systems," Tech. Rep., 2017. [Online]. Available: www.aami.org.